Oscillatory phenomena of compartmentalized bidisperse granular gases

Rui Liu, Yinchang Li, and Meiying Hou
Institute of Physics, Chinese Academy of Sciences, Beijing 100080, China
(Received 8 December 2008; published 19 May 2009)

Compartmentalized bidisperse granular gases are numerically studied. Molecular-dynamics simulations studying granular clock phenomenon in three dimensions are presented, which complement previously reported two-dimensional simulation results. A flux model for binary mixtures is found to give qualitative descriptions for the oscillations, with no undetermined parameters or functions. Two different states, a degenerate oscillatory state and a state with large particles segregated and small particles homogeneously distributed, are found in our simulations. These features reveal a much more complex phase diagram for the system, which challenges the existing theoretical models.

DOI: 10.1103/PhysRevE.79.052301 PACS number(s): 45.70.Qj

Granular systems, in which ordinary thermal fluctuations do not play a role, often exhibit various ordered patterns. Patterns form when the systems turn out to be in multiple metastable steady states, which are far from equilibrium. Spatial ordered structures, such as regular surface patterns, oscillons, segregation structures, etc., have been observed in different kinds of granular systems [1]. Recently, another fascinating phenomenon, oscillation, was also numerically predicted for a binary granular gas in a two-compartment (TC) setup [2,3] and was observed in later reported experiments [4–6]. This so-called granular clock phenomenon may greatly enrich our understanding of the nonequilibrium properties of granular systems.

The TC setup, as shown in Fig. 1(a), was borrowed from the concept of Maxwell's demon. In this setup, a demon state, i.e., segregation of slow and fast-moving particles, was successfully realized with monodisperse inelastic grains [7–10]. For such a monodisperse granular gas, the clustering dynamics and the bifurcation instabilities were well explained by several flux models [8,9,11,12]. Later Mikkelsen *et al.* [13,14] placed binary granular mixtures (large and small steel beads) into a similar system and experimentally showed a competitive clustering phenomenon between the two compartments. They generalized the flux model of Eggers [8] to bidisperse granular gases (referred to as GF model below) to explain the observed phenomena. Though they found no oscillatory states either in their experiments or their numerical results, two later papers predicted this so-called granular clock phenomenon in two-dimensional (2D) systems through molecular-dynamics simulations and theoretical models: Costantini *et al.* [2] simulated systems of smooth hard disks with equal sizes but different masses and developed a mean field theory; while Lambiotte *et al.* [3] simulated those with different sizes but equal masses and suggested a four-ODE description. Miao *et al.* [4] first observed the oscillatory phenomenon experimentally using millets and mung beans, which were different in both size and mass. However, they claimed no oscillation for large and small beads of same material. Viridi *et al.* [5] later observed such an oscillation with large and small glass beads in a quasi-2D system. They adopted the model of Lambiotte *et al.* to explain their results. Our recent results [6] showed the existence of oscillation of glass and steel beads with equal sizes in a three-dimensional (3D) system, and a phenomenological model was raised to show the instability as a supercritical Hopf bifurcation. However, none of the above models obtained quantitative agreements with experimental results and some features we will report here have not been discovered by these models either.

According to all the reported results and accumulated experimental data, we know that oscillations would occur for mixtures of beads with either different masses, different sizes, or even with different coefficients of restitution, under conditions of proper number ratios of beads and proper driving velocity of the bottom plate. With many controlling parameters of such a system, a detailed and complete study by experiments would be rather difficult. Numerical study in this case becomes a necessary supplement. Nonetheless, works on the granular clock in 3D simulations have never been reported, despite the fact that experiments are usually done in 3D, and none of the above theoretical models obtained quantitative agreements with experimental results. In

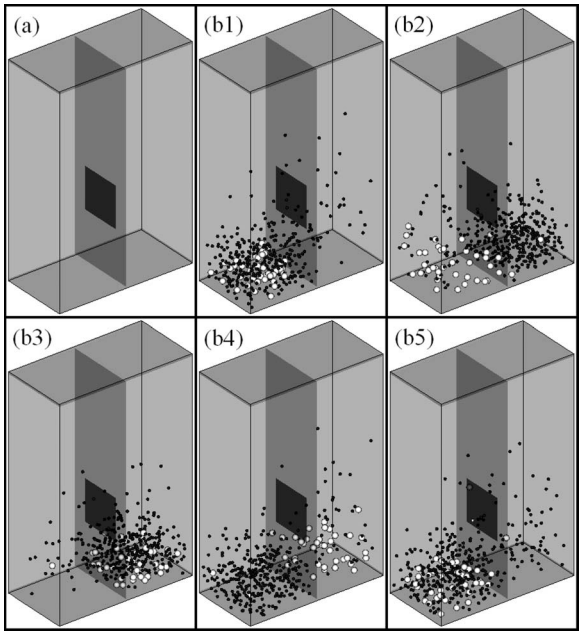

FIG. 1. The TC container (a) and snapshots of an oscillatory state (b1)–(b5) obtained in simulation with 360 small (black) and 40 large (white) beads.

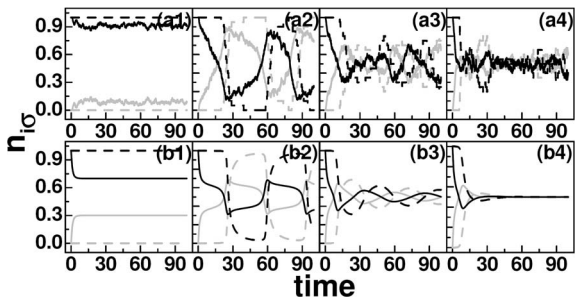

FIG. 2. Simulation results (a1)–(a4) and the corresponding states (b1)–(b4) obtained by the GF model for $\Psi=19$: asymmetrical clustering state at $V_b=0.64$ (a1) and $D=148$ (b1), oscillation at $V_b=0.72$ (a2) and $D=144$ (b2), damped oscillation at $V_b=0.80$ (a3) and $D=138$ (b3), soon reached homogeneous state at $V_b=0.88$ (a4) and $D=134$ (b4); dark solid n_{1l}, gray solid n_{1r}, dark dashed n_{2l}, and gray dashed n_{2r}.

this Brief Report, to study the population of grains in compartmentalized bidisperse granular gases, we have employed 3D event-driven molecular-dynamics simulations and reconsidered the GF model for a better theoretical description. We have not only successfully reproduced oscillation phenomena by our simulation and by the slightly modified GF model, but also obtained phases in simulation.

The simulation method that we use is a standard event-driven algorithm for 3D systems. The particles are taken as hard spheres that deformations are ignored while colliding. Particle-particle and particle-wall collisions are considered as instantaneous events. Between the two events the particles move freely keeping parabolic paths under gravitational acceleration g. At an event of collision the velocities of the particles after contact are computed from the velocities just before the contact, according to Newton's laws. An experimental setup with a TC container fastened onto a shaker is simulated. In the container there are small and large smooth hard spheres, with radius r_i, mass m_i, and total number N_i, respectively ($i=1$ for smaller spheres and $i=2$ for larger ones). Number ratio between the two species is defined as $\Psi=N_1/N_2$. A real occupation state is represented by the numbers of both species in the left and right compartments, i.e., $\{(N_{1l},N_{2l}),(N_{1r},N_{2r})\}$. For convenience, define $N=N_1+N_2$, $\phi_i=N_i/N$, and $n_{i\sigma}=N_{i\sigma}/N_i$, where σ denotes $l(r)$ for the left (right) compartment. The two compartments of the container, with ground area $50r\times 50r$ (in x-y plane) and height $150r$ (z direction) for each, are connected by a rectangular hole with width $W=30r$ and height $H=30r$, centered at $z=50r$. Here r is a scaling length, whose value is set as the radius of the small particles r_1. The bottom of the container is vibrated vertically with adjustable velocity V_b (dimensionless in unit $\sqrt{4gr}$) in a saw-tooth manner. The normal coefficients of restitution ϵ for particle-particle and particle-wall collisions are taken to be constant and both are set to 0.90.

The upper panel of Fig. 2, (a1)–(a4), shows our simulation results for a fixed number ratio $\Psi=19$ (or $\phi_2=0.05$) and $N=400$. The shaking strength increases from $V_b=0.64$ for (a1) to $V_b=0.88$ for (a4). When the shaking is weak, most of the beads tend to be clustered in one of the two compartments, leaving few fast-moving ones in the other, and the system stays in an asymmetrical clustering (ASC) state stably. However, in which compartment particles would assemble, is sensitive to the initial distribution of the beads, and competitive clustering phenomenon may be observed in this regime [13,14]. For moderate shaking, the oscillatory (OSC) state is observed [see Fig. 2 (a2)], same as what we observed in our previous experiments [6]: the large (heavy) particles are more likely to stay near the bottom and transfer energy (or heat) to the small (light) ones. If the vibration velocity is proper, the small (light) particles, lifted up by the large (heavy) ones, have chance to go through the hole and cool down when clustered in the other compartment. Once most of the small (light) particles have emigrated, the large (heavy) ones, without any loads, are pumped high enough by the bottom plate and are able to jump through the hole. The same cycle will repeat to let particles jump from the other compartment back to the original cell. Population oscillation of small and large particles between the two compartments is observed with a phase shift between the large (heavy) beads and the small (light) ones. When the shaking becomes strong enough, the oscillation damps [Fig. 2 (a3)] and finally reaches a homogenous (HOM) state that particles populate equally in the two compartments as is shown in Fig. 2 (a4).

All these results above are similar to previously reported 2D results [2,3]. We would therefore like to use similar models used in the 2D case to our system. Here we review the GF model used by Mikkelsen *et al.* [14]. This GF model is based on several assumptions: (1) In either compartment, energy equipartition is valid between species, so that both species share a common granular temperature T_σ (σ denotes either of the two compartments); (2) each species has a barometric height distribution, therefore the pressure for each species in such a granular gas has a distribution as $p_{i\sigma}(z)=(N_{i\sigma}m_ig/\Omega)e^{-m_igz/k_BT_\sigma}$, where Ω is the ground area of each compartment; (3) Maxwellian and isotropic velocity distribution is assumed, i.e., $\langle v_{\alpha i}^2\rangle=k_BT_\sigma/m_i$, and $\langle|v_{\alpha i}|\rangle=\sqrt{2k_BT_\sigma/\pi m_i}$, where α denotes x,y,z. The balance between the dissipation and energy input determines the granular temperature of each box, $k_BT_\sigma=v_b^2\mu_\sigma/[16\pi(1-\epsilon^2)^2]$, where the explicit form of function $\mu_\sigma(N_{1\sigma},N_{2\sigma})$ could be found in Ref. [14]. Since this model requires barometric height distributions for either species, the fact that heavy particles are more likely to stay near the bottom would be self-evident. This implies a possible description for the OSC state.

The flux function is a key element for such a flux model. Considering that ΔN_i particles of species i hit an elastic rigid wall and rebound from it in a rather short time Δt. For an area with width W and height H in the wall, we can calculate the force on the area with the pressure distribution, simply $f=W\int_h^{h+H}p_{i\sigma}(z)dz$, where h is the bottom height of the hole. The impulse $f\cdot\Delta t$ supplies the particles with momentum $\Delta N_i 2m_i\langle|v_{xi}|\rangle$. If such a $W\times H$ area is excavated, all the ΔN_i particles will flow out through the hole during the time period Δt. Then the flow rate is

$$F^i(N_{1\sigma},N_{2\sigma})=\frac{\Delta N_i}{\Delta t}=\frac{f}{2m_i\langle|v_{xi}|\rangle}.$$

With known $p_{i\sigma}(z)$ and $\langle|v_{xi}|\rangle$, a similar flux function to Mikkelsen *et al.*'s can be obtained,

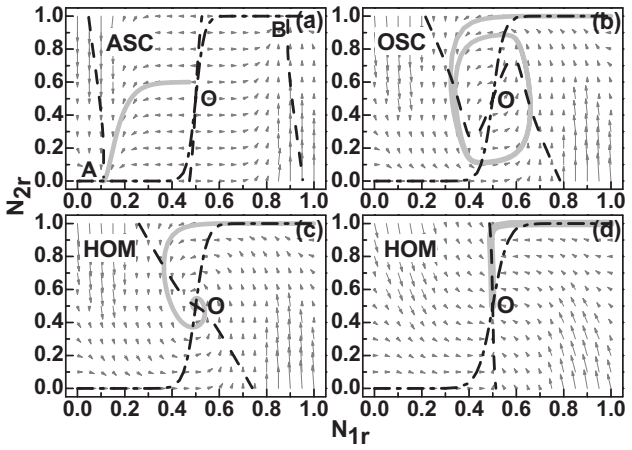

FIG. 3. Flow diagrams $(\frac{dn_{1r}}{dt}, \frac{dn_{2r}}{dt})$: (a) $D=192$, (b) $D=142$, (c) $D=137$, and (d) $D=100$; dashed lines for $\frac{dn_{1r}}{dt}=0$ and dash-dot for $\frac{dn_{2r}}{dt}=0$; gray lines show specific tracks of the system as illustrations, while the evolving direction is just along the vector field.

$$F^i(N_{1\sigma},N_{2\sigma}) = KN_{i\sigma}\sqrt{\frac{\mu_\sigma}{m_i}}e^{-Dm_i/\mu_\sigma}(1-e^{-\eta Dm_i/\mu_\sigma}),$$

where $K=\frac{Wv_b}{8\sqrt{2}\Omega(1-\epsilon^2)}$, $D=\frac{16\pi gh(1-\epsilon^2)^2}{v_b^2}$, $\eta=H/h$, and h is the bottom height of the excavated area. D is an important controlling parameter indicating the ratio of energy loss and energy input, as Mikkelsen *et al.* [14] have pointed out.

Using this flux function, we rebuild the coupling dynamical equations of the system for species $i=1,2$ as follows:

$$\frac{dn_{il}}{dt} = -\frac{dn_{ir}}{dt} = -F^i(n_{1l},n_{2l}) + F^i(n_{1r},n_{2r}).$$

With given initial conditions for $\{(n_{1l},n_{2l}),(n_{1r},n_{2r})\}$, we are able to predict how the system evolves. Calculations show that this flux model, with different shaking strength, may exhibit three possible steady states: ASC, OSC, and HOM [shown in the lower panel of Fig. 2, (b1)–(b4)]. Oscillation occurs at an intermediate value of D, which is between the regime of ASC and that of HOM. All the curves agree qualitatively well with our simulation results.

Within this flux model, the net flux $\frac{dn_{ir}}{dt}$ for either species in one of the compartments at different values of D in the range of ASC, OSC, and HOM regimes, respectively, is calculated and the flow diagrams are given in the n_{1r}-n_{2r} plane shown in Fig. 3. When D is large that the shaking velocity is low, there are three fixed points for the system among which A and B are stable and O is unstable. The system stays in the ASC regime and reaches its final steady state at point A or B, depending on where it is initialized [Fig. 3(a)]. As D becomes smaller, shaking strength is stronger, and a limit cycle appears. This limit cycle is expected to be stable and the system oscillates [Fig. 3(b)]. When D is even smaller, the center O becomes a stable fixed point, and the system is always led to this point, i.e., reaching a HOM state [Figs. 3(c) and 3(d)].

As shown above, we have successfully obtained using our 3D simulations and the GF model the OSC state, showing

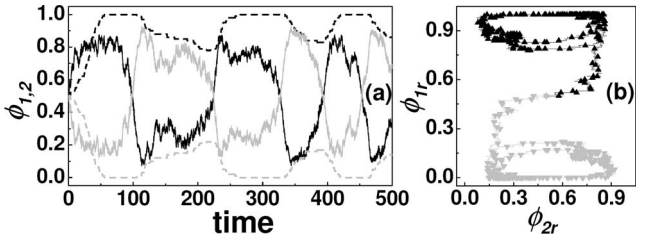

FIG. 4. Oscillatory curves of the d-OSC state for $\Psi=3$ at $V_b=0.60$ (a) (dark solid n_{1l}, gray solid n_{1r}, dark dashed n_{2l}, and gray dashed n_{2r}) and the corresponding phase orbit with two possible branches on the n_{1r}-n_{2r} plane (b).

similar oscillatory curves with nearly the same values of oscillation period (in Fig. 2) with different corresponding values of v_b (in simulations) and D (in GF model). Moreover, it is interesting to see that in our 3D simulations, some different states are observed, which have not been described by either the GF model or any previous models.

Choosing a much smaller number ratio, say $\Psi=3$ (or $\phi_2=0.25$), we find a degenerate oscillatory (d-OSC) state, as shown in Fig. 4. In this state, the large particles mainly stay in one of the compartments with only a small number of them participating in the oscillation, while most of the small ones oscillate between the two compartments. In this case comparing with the situation in Fig. 2, there are more large particles so that the dissipation due to large-large particle collisions is as significant as large-small particle collisions. Therefore the change in number of small particles in the compartment cannot affect the velocity of the remaining large particles significantly that the large particles remain in a so-called degenerate oscillation state. Although the whole system is still in an oscillatory state, its phase orbit in the n_{1r}-n_{2r} plane has already taken a topological transition: the single limit cycle breaks into doubly degenerate ones [see Fig. 4(b)]. This is interesting and none of the previous models have ever predicted it.

To know more about the d-OSC state, a detailed phase diagram [15] is obtained by simulations, as shown in Fig. 5. There appears the d-OSC regime next to OSC regime, when

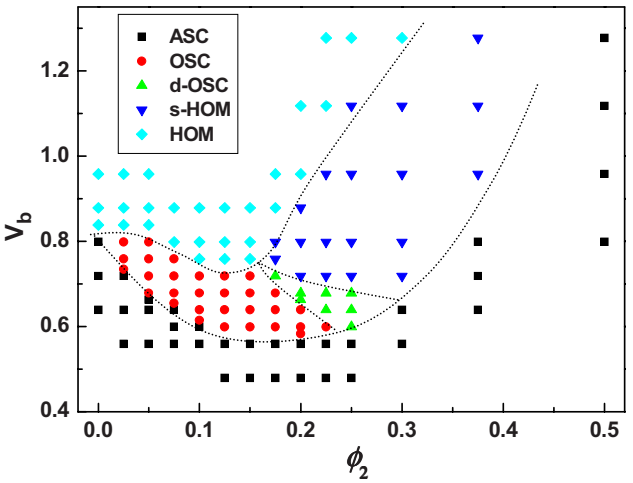

FIG. 5. (Color online) Phase diagram by molecular-dynamics simulations with $N=400$.

the number fraction of the large particles ϕ_2 is less than 0.3. We see that as the number fraction ϕ_2 increases, the OSC regime gradually gives place to d-OSC regime, and finally disappears. Within the range that both of these oscillatory states coexist, the OSC regime is found at lower driving velocity V_b comparing to that in the d-OSC regime. This means an OSC state requires less energy injection than a d-OSC state. It is interesting to note that proper weaker shaking can make nearly all the particles oscillate between compartments, while stronger shaking cannot. Also observed is a concomitant state of the d-OSC state: the small beads are homogeneously distributed (s-HOM), while the large ones show an asymmetric segregation. The existence of s-HOM state can be understood as a state originating from the d-OSC regime by increasing driving velocity V_b.

Finally we would like to discuss the stability of the d-OSC state for the corresponding regime is narrow in the phase diagram same as for the OSC regime [2,3,6]. Though all the models do have limit cycle solutions for the OSC regime, none of them are quantitatively accurate and can hardly predict or ensure the state being stable. In our simulations, we tried running the program for many cycles, no obvious damp was observed in the results during the time of at least 15 oscillations for both the OSC and d-OSC states, and the system could cross the same point for many cycles in the n_{1r}-n_{2r} plane. We also tested the system with various initial distributions, i.e., it was set at different points, inside or outside the limit cycle that we assumed, at the beginning. We found that it returned to the cyclic orbit wherever it started, and this made us believe that the d-OSC state should not be a transient state.

In conclusion, we demonstrate that the ASC, OSC, and HOM states of bidisperse granular gases in a TC system can be reproduced by 3D molecular-dynamics simulations and the GF model, and more interestingly two different states, d-OSC and s-HOM, are found in our simulations. Further theoretical modeling and experimental studies are needed for better understanding of these phenomena.

This work was supported by CNSF Grant Nos. 10720101074 and 10874209, and by CAS Grant Nos. KKCX1-YW-03 and KJCX2-YW-L08.

[1] I. S. Aranson and L. S. Tsimring, Rev. Mod. Phys. **78**, 641 (2006).
[2] G. Costantini, D. Paolotti, C. Cattuto, and U. M. B. Marconi, Physica A **347**, 411 (2005).
[3] R. Lambiotte, J. M. Salazar, and L. Brenig, Phys. Lett. A **343**, 224 (2005).
[4] T. Miao, Y. Liu, F. Miao, and Q. Mu, Chin. Sci. Bull. **50**, 726 (2005).
[5] S. Viridi, M. Schmick, and M. Markus, Phys. Rev. E **74**, 041301 (2006).
[6] M. Hou, H. Tu, R. Liu, Y. Li, K. Lu, P. Y. Lai, and C. K. Chan, Phys. Rev. Lett. **100**, 068001 (2008).
[7] T. Shinbrot and F. J. Muzzio, Nature (London) **410**, 251 (2001).
[8] J. Eggers, Phys. Rev. Lett. **83**, 5322 (1999).
[9] J. J. Brey, F. Moreno, R. García-Rojo, and M. J. Ruiz-Montero, Phys. Rev. E **65**, 011305 (2001).
[10] K. van der Weele, D. van der Meer, M. Versluis, and D. Lohse, Europhys. Lett. **53**, 328 (2001).
[11] A. Lipowski and M. Droz, Phys. Rev. E **65**, 031307 (2002).
[12] H. Hinrichsen and D. E. Wolf, *The Physics of Granular Media* (Wiley-VCH Verlag GmbH & Co. KGaA, Weinheim, 2004).
[13] R. Mikkelsen, D. van der Meer, K. van der Weele, and D. Lohse, Phys. Rev. Lett. **89**, 214301 (2002).
[14] R. Mikkelsen, D. van der Meer, K. van der Weele, and D. Lohse, Phys. Rev. E **70**, 061307 (2004).
[15] Here we do not consider the state that no particles can go through the hole for very weak shaking.